Reactions of Aryl Phenylacetates with Secondary Amines in MeCN. Structure−Reactivity Relationship in the Ketene-Forming Eliminations and Concurrent E2 and E1cb Mechanisms

Bong Rae Cho,* Yong Kwan Kim, and Choon-Ock Maing Yoon

*Contribution from the Department of Chemistry, Korea University,
1-Anamdong, Seoul 136-701, Korea*

Abstract: Elimination reactions of aryl esters of arylacetic acids **1** and **2** promoted by R_2NH in MeCN have been investigated kinetically. The reactions are second-order and exhibit $\beta = 0.44-0.84$, $|\beta_{lg}| = 0.41-0.50$, and $\rho_H = 2.0-3.6$. Brønsted β and $|\beta_{lg}|$ decrease with the electron-withdrawing ability of the β-aryl substituent. Hammett ρ_H values remain nearly the same, but the $|\beta_{lg}|$ value increases as the base strength becomes weaker. Both ρ_H and β decrease with the change of the leaving group from 4-nitrophenoxide to 2,4-dinitrophenoxide. The results are consistent with an E2 mechanism and a reaction coordinate with a large horizontal component corresponding to proton transfer. When the base−solvent system is changed from R_2NH−MeCN to $R_2NH/R_2NH_2{}^+$−70 mol % MeCN(aq), the Brønsted β, ρ_H, and $|\beta_{lg}|$ decrease. Finally, the ketene-forming elimination reactions from *p*-nitrophenyl *p*-nitrophenylacetate promoted by $R_2NH/R_2NH_2{}^+$ buffers in 70 mol % MeCN(aq) have been shown to proceed by concurrent E2 and E1cb mechanisms.

Extensive studies of structure−reactivity relationships in elimination reactions have led to a qualitative understanding of the relationship between the reactant structure and the E2 transition state.[1−8] Most of the results from these studies have been interpreted with More-O'Ferrall−Jencks energy diagram by assuming similar effects for the parallel and perpendicular motion.[5−8] In contrast, much less is known about the effects of the reactant structure on the E1cb-like transition state, where the effects in the two directions are different.[9−11]

Perhaps an even more important problem in elimination mechanism studies may be the mechanistic borderlines. It is conceivable that the change of the elimination mechanism may occur by "merging" of the transition states, i.e., the concerted mechanism is enforced by the change in the lifetime of the intermediate. The mechanistic changes from E2 to E1cb for eliminations reactions of (2-arylethyl)ammonium ions[9] and 9-(2-chloro-2-propyl)fluorene[12] have been concluded to be of this type. Alternatively, the change in mechanism may also involve

two concurrent mechanisms having different transition state structures. A change in experimental condition or reactant structure may lower the energy of one of the transition states, which may in turn induce a shift in the major reaction pathway. Such examples have been reported in the E2 and E1 borderline for the methoxide-promoted eliminations from 2-chloro-2-methyl-1-phenylpropane[13] and *N*-(arylsulfonoxy)-*N*-alkylbenzylamines[14] as well as for the solvolytic elimination of 9-(1-X-ethyl)fluorenes.[15] However, no clear evidence for the concurrent E2 and E1cb mechanisms has been reported. Although the small isotope effect observed in eliminations from 1-(2-chloro-2-propyl)indene has been interpreted with parallel E2 and E1cb mechanisms, the result could also be attributed to a reverse stepwise preassociation mechanism.[16]

One of the promising compounds that may be useful to investigate both of these problems is the aryl esters of phenylacetic acids. It has been reported that the base-catalyzed hydrolysis of aryl *p*-nitrophenylacetates[17−22] and other activated esters[22] proceed by an E1cb elimination to afford the ketene

⊗ Abstract published in *Advance ACS Abstracts,* December 15, 1996.
(1) Saunders, Jr. W. H.; Cockerill, A. F. *Mechanism of Elimination Reactions*; Wiley: New York, 1973.
(2) Bartsch, R. A.; Zavada, J. *Chem. Rev.* **1980**, *80*, 453−494.
(3) Lowry, T. H.; Richardson, K. S. *Mechanism and Theory in Organic Chemistry*; Harper and Row: New York, 1987; (a) pp 214−218, (b) pp 591−560, (c) pp 640−644.
(4) Hoffman, R. V.; Bartsch, R. A.; Cho, B. R. *Acc. Chem. Res.* **1989**, *22*, 211−217.
(5) Cho, B. R.; Kim, K. D.; Lee, J. C.; Cho, N. S. *J. Am. Chem. Soc.* **1988**, *110*, 6145−6148.
(6) Cho, B. R.; Jung, J.; Ahn, E. K. *J. Am. Chem. Soc.* **1992**, *114*, 3425−3458 and references cited therein.
(7) Gandler, J. R. In *The Chemistry of Double Bonded Functional Groups*; Patai, S., Ed.; Chichester: New York, 1989; Vol. 2, Part 1, pp 734−797.
(8) Jencks, W. P. *Chem. Rev.* **1985**, *85*, 511−527.
(9) Gandler, J. R.; Jencks, W. P. *J. Am. Chem. Soc.* **1982**, *104*, 1937−1951.
(10) Gandler, J. R.; Yokohama, T. *J. Am. Chem. Soc.* **1984**, *106*, 130−135.
(11) Gandler, J. R.; Storer, J. W.; Ohlberg, D. A. A. *J. Am. Chem. Soc.* **1990**, *112*, 7756−7762.
(12) Thibblin, A. *J. Am. Chem. Soc.* **1988**, *110*, 4582−4586.

(13) Thibblin, A. *J. Am. Chem. Soc.* **1989**, *111*, 5412−5416.
(14) Cho, B. R.; Pyun, S. Y. *J. Am. Chem. Soc.* **1991**, *113*, 3920−3924.
(15) Meng, Q.; Thibblin, A. *J. Am. Chem. Soc.* **1995**, *117*, 9399−9407.
(16) Olwegard, M.; McEwen, I.; Thibblin, A.; Ahlberg, P. *J. Am. Chem. Soc.* **1985**, *107*, 7494−7499.
(17) Holmquist, B.; Bruice, T. C. *J. Am. Chem. Soc.* **1969**, *91*, 3003−3006.
(18) Tagaki, W.; Kobayashi, S.; Kurihara, K.; Kurashima, K.; Yoshida, Y.; Yano, J. *J. Chem. Soc., Chem. Commun.* **1976**, 843−845.
(19) Chandrasekar, R.; Venkatasubramanian, N. *J. Chem. Soc., Perkin Trans. 2* **1982**, 1625−1631.
(20) Broxton, T. J.; Duddy, N. W. *J. Org. Chem.* **1981**, *46*, 1186−1191.
(21) Chung, S. Y.; Yoh, S. D.; Choi, J. H.; Shim, K. T. *J. Korean Chem. Soc.* **1992**, *36*, 446−452.
(22) (a) Holmquist, B.; Bruice, T. C. *J. Am. Chem. Soc.* **1969**, *91*, 2993−3002. (b) Pratt, R. F.; Bruice, T. C. *J. Am. Chem. Soc.* **1970**, *92*, 5956−5964. (c) Inoue, M.; Bruice, T. C. *J. Am. Chem. Soc.* **1982**, *104*, 1644−1653. (d) Inoue, M.; Bruice, T. C. *J. Org. Chem.* **1982**, *51*, 959−963. (e) Isaac, N. S.; Najem, T. S. *J. Chem. Soc., Perkin Trans. 2* **1988**, 557−562. (f) Douglas, K. T.; Alborz, M.; Rullo, G. R.; Yaggi, N. F. *J. Chem. Soc., Chem. Commun.* **1982**, 242−246. (g) William, A. *J. Chem. Soc., Perkin Trans. 2* **1972**, 808−812. (h) Williams, A.; Douglas, K. T. *Chem. Rev.* **1975**, 627−649.

Table 1. Rate Constants for Aminolysis of Aryl Alkanoates[a] Promoted by R_2NH in MeCN at 25.0 °C

		$10^2 k_2{}^S$, M^{-1} s^{-1} [d]				
base[b]	$pK_a{}^c$	4a	4b	4c	4d	2a[e]
Bz(*i*-Pr)NH	16.8	0.358	0.115	0.060	0.020	0.0004
i-Bu₂NH	18.2	56.2	24.2	15.1	5.40	0.1
i-Pr₂NH[f]	18.5	1.54	1.04	0.620	1.04	0.006
2,6-DMP[g,h]	18.9	113	47.3	29.2	8.50	0.175

[a] [Substrate] = 2.0 × 10⁻⁵ M. [b] [Base] = 8.5 × 10⁻³ to 5.0 × 10⁻¹ M. [c] Reference 36. [d] Estimated uncertainty, ±5%. [e] Estimated from the Charton plot and the steric effect parameter 0.7 for the benzyl group (see text).[24] [f] $10^4 k_2{}^S$ values for the reactions of **3a**, **3b**, **3c**, and **3d** with *i*-Pr₂NH/*i*-Pr₂NH₂⁺ buffer in 70 mol % MeCN(aq) are 1.6, 1.08, 6.16, 5.87 M^{-1} s^{-1}, respectively. [g] *cis*-2,6-Dimethylpiperidine. [h] The $k_2{}^S$ value for the reaction of **3a** with 2,6-DMP is 2.03 × 10⁻⁴ M^{-1} s^{-1}.

intermediate followed by the addition of water under various conditions. It occurred to us that the ketene-forming eliminations may proceed by the E2 mechanism via an E1cb-like transition state if the reactions were conducted under conditions where the carbanion intermediate is destabilized. Concurrent E2 and E1cb mechanisms may also be observed if the reaction conditions are varied so that the energies of the two transition states become almost the same. Accordingly, we have investigated the reactions of aryl esters of substituted phenylacetic acids **1** and **2** with secondary amines in acetonitrile (eq 1). Sterically bulky amines have been employed to avoid the complications that may be caused by the aminolysis of the substrates.
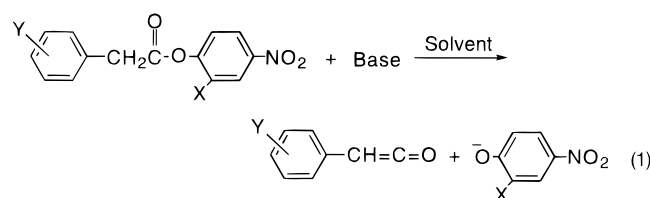
X = H (**1**), NO₂ (**2**)

Y = H (**a**), *p*-MeO (**b**), *m*-Cl (**c**), *m*-NO₂ (**d**), *p*-NO₂ (**e**)

Base-Solvent = R₂NH-MeCN, R₂NH/R₂NH₂⁺- 70 mol % MeCN(aq)

R₂NH = Bz(*i*-Pr)NH, *i*-Bu₂NH, *i*-Pr₂NH, 2,6-DMP

In this work, we have studied the effects of reactant structures upon the ketene-forming eliminations. This reaction provided us with an unusual opportunity to look into the structure−reactivity correlations for the E1cb-like transition state. The concurrent E2 and E1cb reactions have also been observed. The results of these studies are reported here.

Results

Aryl phenylacetates **1** and **2** and aryl alkanoates **3** and **4** were prepared by the literature method.[23] The reactions of **1a** and **2a** with diisopropylamine in MeCN produced *N,N*-diisopropyl-benzamide in 88 and 92% yields, respectively. From the reactions of **1a** and **2a** with *i*-Pr₂NH/*i*-Pr₂NH₂⁺ in 70 mol % MeCN(aq) were obtained *N,N*-diisopropylbenzamide and phe-nylacetic acid as the only products. The yields of the aryloxides as determined by comparison of the UV absorption of the infinity sample of the kinetic runs with those for the authentic samples were in the range 92−98%.

The rates of the reactions of **1** and **2** with R₂NH−MeCN were followed by monitoring the increase in the absorption for the aryloxides at 400 and 426 nm, respectively. In all cases,

clean isosbestic points were noted in the range 286−318 nm. Excellent pseudo-first-order kinetic plots which covered at least 3 half-lives were obtained. For reactions of **1a−d** and **2a−e** with R₂NH, the plots of k_{obs} vs base concentration were straight lines passing through the origin. The slopes were the overall second-order rate constants k_2.

To probe whether the aminolysis reaction may compete with the ketene-forming elimination, the rates of aryloxides production from the reactions of aryl alkanoates **3** and **4** with R₂NH were determined (eq 2). Except for the reaction of **3a** with
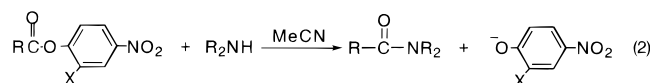
X = H (**3**), NO₂ (**4**)

R = Me (**a**), Et (**b**), *n*-Pr (**c**), *i*-Pr (**d**)

R₂NH = Bz(*i*-Pr)NH, *i*-Bu₂NH, *i*-Pr₂NH, 2,6-DMP

2,6-DMP, **3** did not react with R₂NH under the reaction condition. However, **4** underwent aminolysis with all of the R₂NH employed. The second-order rate constants $k_2{}^S$ for the aminolysis reactions are summarized in Table 1. The rate increased as the basicity of the amine increased but decreased as the steric bulk of the alkyl group increased. The slower rate of aminolysis from **4** with *i*-Pr₂NH than with *i*-Bu₂NH as the base can be attributed to the greater steric requirement of the former.

The plots of log k_2 vs Charton's steric effect parameter ν[24] for the aminolysis of **4** with R₂NH in MeCN are shown in Figure S1 in the Supporting Information. The $k_2{}^S$ values for the reactions of **2** with R₂NH were estimated from the Charton plots by using the steric effect parameter of 0.7 for the benzyl group[24] and are listed in Table 1. In all cases, the $k_2{}^S$ values were negligible compared with the k_2 values (Tables 1 and 2). Therefore, no correction was necessary to obtain the second-order rate constants for eliminations reactions $k_2{}^E$ from k_2. The $k_2{}^E$ values for the ketene-forming eliminations from **1** and **2** promoted by R₂NH in MeCN are summarized in Table 2.

Brønsted plots for eliminations from **1** and **2** are linear with excellent correlation (plots not shown). The β values are in the range 0.44−0.84 and decrease as the electron-withdrawing ability of the substituent and the leaving group ability of the aryloxides increase (Table 3).

The Hammett plots for eliminations from **1a−d** are curvilinear and show downward curvature (Figure 1). Similar plots were observed for the reactions of **2a−e** (plots not shown). The rate data could be correlated with eq 3 using a nonlinear

$$\log(k/k_0) = \rho_H \sigma^- + \tau \sigma^{-2} = (\rho_H + \tau \sigma^-)\sigma^- \qquad (3)$$

regression analysis program,[25] where ρ_H and τ values are the slope of the Hammett plot when Y = H and the proportionality factor by which the ρ value is influenced by the electron-withdrawing ability of the substituents, respectively. For all reactions the correlations between the experimental and the calculated data were excellent, demonstrating the validity of this analysis. Utilizing the computer program, the ρ_H and τ values that best fit with eq 3 have been calculated. The ρ_H and τ values are in the range 2.0−3.6 and −0.43 to −2.3 (Table 4). The values are independent of the base strength but decrease as the pK_a value of the leaving group is decreased (Table 4).

The β_{lg} values are calculated from the rate data and the pK_{lg} values of the leaving group. The $|\beta_{lg}|$ values are in the range

(23) Saigo, K.; Usui, M.; Kikuchi, K.; Shimada, E.; Mukaiyama, T. *Bull. Chem. Soc. Jpn.* **1977**, *50*, 1863−1866.

(24) Charton, M. *J. Am. Chem. Soc.* **1975**, *97*, 1552−1556.
(25) MicroCal Origin Version 3.5, MicroCal Software, Inc., Northampton, MA, 1991.

Table 2. Rate Constants for Ketene-Forming Eliminations from $YC_6H_4CH_2CO_2Ar^a$ Promoted by R_2NH in MeCN at 25.0 °C

| base[b] | $10^2 k_2^E$, M^{-1} s^{-1} [c] | | | | k_2^E, M^{-1} s^{-1} [c] | | | | |
	1a	1b	1c	1d	2a	2b	2c	2d	2e
Bz(*i*-Pr)NH	0.260	0.040	2.81	12.4	0.264	0.0874	2.32	10.5	60.0
i-Bu$_2$NH	3.80	0.575	38.9	97.7	3.02	0.995	13.4	60.3	260
i-Pr$_2$NH	6.58	1.14	59.4	166	4.17	1.39	18.8	77.6	346
2,6-DMP[d]	14.2	2.21	146	350	7.10	2.96	35.6	135	508

[a] [Substrate] $= 2.0 \times 10^{-5}$ M. [b] [Base] $= 1.0 \times 10^{-3}$ to 2.0×10^{-1} M. [c] Estimated uncertainty, ±5%. [d] *cis*-2,6-Dimethylpiperidine.

Table 3. Effect of Aryl Substituents upon Brønsted β and β_{lg} Values for Eliminations from $YC_6H_4CH_2CO_2Ar$ Promoted by R_2NH in MeCN at 25.0 °C

| | β | | |
Y	Ar = 4-nitrophenyl	Ar = 2,4-dinitrophenyl	$\beta_{lg}{}^a$
p-CH$_3$O	0.84 ± 0.01	0.72 ± 0.02	−0.50
H	0.82 ± 0.01 (0.77 ± 0.03)[b]	0.69 ± 0.04	−0.43
m-Cl	0.81 ± 0.02	0.56 ± 0.02	−0.41
m-NO$_2$	0.68 ± 0.03	0.52 ± 0.02	−0.41
p-NO$_2$	− (0.66 ± 0.07)[b]	0.44 ± 0.01	−

[a] The base was Bz(*i*-Pr)NH. [b] Calculated with the k_2^E values in Table 5 for eliminations from **1a** and **1e** promoted by $R_2NH/R_2NH_2^+$ buffers in 70 mol % MeCN(aq) at 25.0 °C.
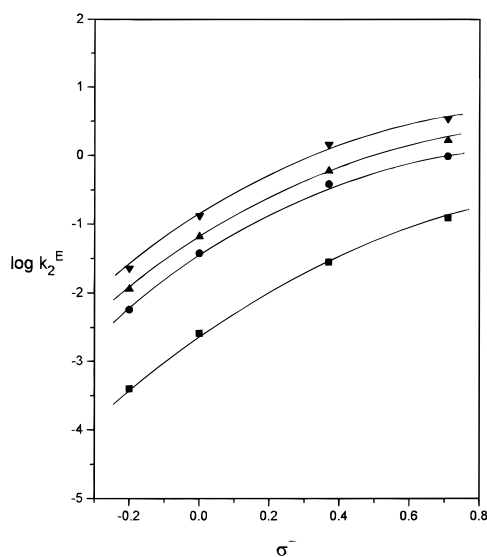
Figure 1. Hammett plots for the ketene-forming eliminations from *p*-nitrophenyl arylacetate **1** [$YC_6H_4CH_2COOC_6H_4$-*p*-NO_2] promoted by R_2NH in MeCN at 25.0 °C. The data are from Table 2, and the lines were calculated by nonlinear regression analysis by using eq 3 (see text) [R_2NH = Bz(*i*-Pr)NH (■), *i*-Bu$_2$NH (●), *i*-Pr$_2$NH (▲), 2,6-DMP (▼)].

Table 4. Effect of Base Strength upon the ρ_H, τ, and β_{lg} Values for Eliminations from $YC_6H_4CH_2CO_2C_6H_3$-2-X-4-NO_2 Promoted by R_2NH in MeCN at 25.0 °C

| | X = H | | X = NO$_2$ | | |
base	ρ_H	τ	ρ_H	τ	$\beta_{lg}{}^a$
Bz(*i*-Pr)NH	3.5 ± 0.1	−2.2 ± 0.1	2.0 ± 0.1	−0.44 ± 0.07	−0.43
i-Bu$_2$NH	3.3 ± 0.1	−1.9 ± 0.1	2.1 ± 0.1	−0.43 ± 0.10	−0.40
i-Pr$_2$NH	3.6 ± 0.1	−2.3 ± 0.1	2.1 ± 0.1	−0.43 ± 0.08	−0.38
2,6-DMP[b]	3.5 ± 0.1	−1.6 ± 0.2	2.1 ± 0.1	−0.48 ± 0.10	−0.37

[a] Y = H. [b] *cis*-2,6-Dimethylpiperidine.

0.37−0.50 and decrease as the electron-withdrawing ability of the aryl substituent and the pK_a value of the base increase (Tables 3 and 4).

In contrast to the reactions of **1a−d** and **2a−e**, the k_{obs} for the reactions of **1e** with R_2NH in MeCN showed a curvilinear relationship with the base concentration (Figure S2). However,

the kinetic data cannot be analyzed accurately because the R_2-NH_2^+ concentration increases as the reaction proceeds (eq 4).

$$k_{obs} = k_2^E[B] + \frac{k_1 k_2[B]}{k_{-1}[BH^+] + k_2} \quad (4)$$
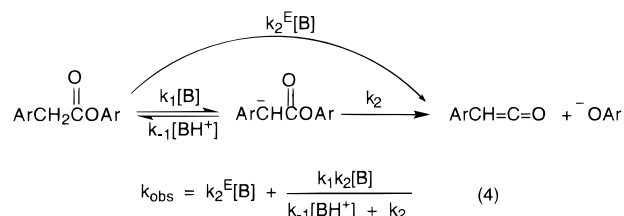
Hence the base−solvent system was changed to $R_2NH/R_2NH_2^+$ buffer in 70 mol % MeCN(aq). Large excess amount of the buffer was used to ensure that the $R_2NH_2^+$ concentration remained constant. The kinetic experiments were carried out as described above. A typical plot of the k_{obs} vs buffer concentration for the reaction of **1a** with *i*-Pr$_2$NH/*i*-Pr$_2$NH$_2^+$ buffer in 70 mol % MeCN(aq) is shown in Figure S3. For all reactions, the plots showed downward curvature. The curvature is essentially independent of the substrate structure, indicating that it does not represent a change in rate-limiting step but may be caused by the buffer association. The buffer association constant K_{assoc} was estimated from the negative deviation of the rate data for reactions of **1a** with $R_2NH/R_2NH_2^+$ buffers by assuming that it occurs due to the formation of kinetically inactive hydrogen-bonded complexes, $R_2NH_2^+ \cdots NHR_2$.[26] The K_{assoc} values are 6.5, 6.0, 7.3, and 20 M^{-1} for benzylisopropylamine, diisobutylamine, diisopropylamine, and 2,6-dimethylpiperidine, respectively. The much larger K_{assoc} value for the latter may in parts be attributed to the smaller steric requirement and lower solubility of its buffer in 70 mol % MeCN(aq). The second-order rate constants k_2^E for eliminations from **1a−d** and **2a** promoted by $R_2NH/R_2NH_2^+$ buffer in 70 mol % MeCN(aq) were obtained from the slopes of the plots of the k_{obs} vs "free" buffer concentration calculated with the K_{assoc} values. The plots are linear for all reactions. No correction for the competing aminolysis reaction has been made to the k_2^E values because the rates of aminolysis of **3a−d** are negligible (see footnote in Table 1). The k_2^E values are summarized in Table 5.

Figure 2 shows the plot of the k_{obs} for the reactions of **1e** with *i*-Pr$_2$NH/*i*-Pr$_2$NH$_2^+$ buffer vs free buffer concentration. The data were analyzed with a nonlinear regression analysis program[27] by assuming that the reaction proceeds by concurrent E2 and E1cb mechanisms. Utilizing the computer program, the k_2^E, k_1, and k_{-1}/k_2 values that best fit with eq 4 were calculated, and the plots were dissected into the E2 and E1cb reaction components (Figure 2). In all cases, the correlations between the calculated and the experimental data are excellent (Figures S4−S6). Calculated k_2^E, k_1, and k_{-1}/k_2 values are summarized in Table 5.

Brønsted plots for eliminations from **1a** and **1e** promoted by $R_2NH/R_2NH_2^+$ buffer in 70 mol % MeCN(aq) are straight lines

(26) Keeffe, J. R.; Jencks, W. P. *J. Am. Chem. Soc.* **1983**, *105*, 265−279.

(27) A data analysis and graphical plotting program "GENPLOT", Computer Graphic Service, Lansing, New York, 1989.

694 *J. Am. Chem. Soc., Vol. 119, No. 4, 1997*

Cho et al.

Table 5. The k_2^E, k_1, and k_{-1}/k_2 Values for Elimination from $YC_6H_4CH_2COOC_6H_4\text{-}p\text{-}NO_2{}^a$ Promoted by $R_2NH/R_2NH_2{}^+$ Buffers in 70 mol % MeCN(aq) at 25.0 °C

	Y = H	Y = $p\text{-}NO_2$		
R_2NH^b	$10^2 k_2^{E,c}$ $M^{-1} s^{-1}$	$k_2^{E,c,d}$ $M^{-1} s^{-1}$	$k_1{}^{c,d}$ $M^{-1} s^{-1}$	$k_{-1}/k_2{}^{c,d}$
Bz(i-Pr)NH	0.173	0.58	1.81	387
i-Bu$_2$NH	2.00	3.46	18.0	240
i-Pr$_2$NH	4.00^e	6.41	37.0	202
2,6-DMP^f	6.60	16.0	55.7	142

^{a} [Substrate] = 2.0×10^{-5}. ^{b} [Buffer] = 1.0×10^{-3} to 2.0×10^{-1} M. ^{c} Estimated uncertainty, $\pm 5\%$. ^{d} Calculated from the k_{obs} values using eq 4 by nonlinear regression analysis (see text). ^{e} The k_2^E values for reactions of **1b–d** and **2a** with i-Pr$_2$NH/i-Pr$_2$NH$_2{}^+$ buffer in 70 mol % MeCN(aq) are 0.016, 0.200, 0.635, and 0.676 $M^{-1} s^{-1}$ for **1b**, **1c**, **1d**, and **2a**, respectively. ^{f} *cis*-2,6-Dimethylpiperidine.
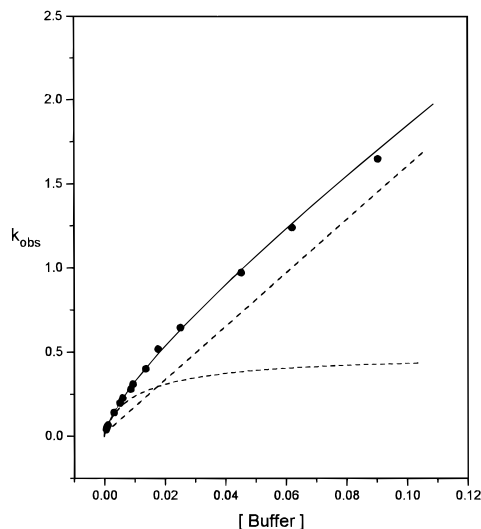
Figure 2. Dependence of k_{obs} vs free buffer concentration for the ketene-forming eliminations from *p*-nitrophenyl *p*-nitrophenylacetate **1e** [$p\text{-}O_2NC_6H_4CH_2COOC_6H_4\text{-}p\text{-}NO_2$] promoted by i-Pr$_2$NH/i-Pr$_2NH_2{}^+$ in 70 mol % MeCN(aq) at 25.0 °C. The closed circles show experimental data and the solid line shows the computer-fitted curve by using eq 4 (see text). The curve is dissected into the E2 and E1cb reaction components (dashed lines).

Table 6. Solvent Effect on the Ketene-Forming E2 Reaction of $YC_6H_4CH_2COOC_6H_4\text{-}p\text{-}NO_2$

solvent	MeCN	70 mol % MeCN(aq)
rel rate^{a,b}	1	0.6
$\rho_H{}^b$	3.6 ± 0.1	1.8 ± 0.1
β^c	0.82 ± 0.01	0.77 ± 0.03
$\beta_{lg}{}^{a,c}$	-0.38	-0.26

^{a} Y = H. ^{b} Base–solvent = i-Pr$_2$NH in MeCN and i-Pr$_2$NH/i-Pr$_2$NH$_2{}^+$ buffer in 70 mol % MeCN(aq), respectively. ^{c} Base–solvent = R_2NH in MeCN and $R_2NH/R_2NH_2{}^+$ buffer in 70 mol % MeCN(aq), respectively.

with excellent correlations (plots not shown). Since the pK_a values of $R_2NH_2{}^+$ in 70 mol % MeCN(aq) are not known in the literature, the $(pK_a)_{MeCN}$ values have been used to calculate the β value.[28,29] The β values for the k_2^E processes are 0.77 ± 0.03 and 0.66 ± 0.07 for **1a** and **1e**, respectively (Tables 3 and 6).

A Hammett plot for eliminations from **1a–e** promoted by $R_2NH/R_2NH_2{}^+$ buffer in 70 mol % MeCN(aq) is depicted in

(28) Coetzee has shown that the $\Delta pK_a = (pK_a)_{MeCN} - (pK_a)_{H_2O}$ values for the structurally similar amines are nearly the same.[29] Therefore, the differences in the pK_a values of the R_2NH employed in this study should be nearly the same in both MeCN and 70 mol % MeCN(aq). Accordingly, no correction has been made to the $(pK_a)_{MeCN}$ values in the Brønsted plots of the rate data measured in 70 mol % MeCN(aq).
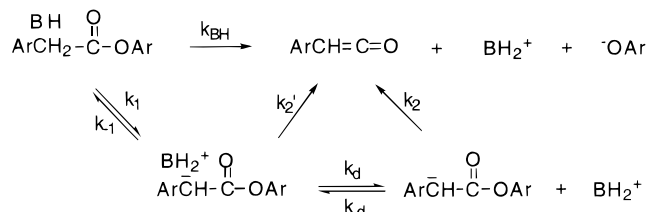
Scheme 1

Figure S7. In contrast to the reactions of **1** and **2** with R_2NH in MeCN, the plot is linear, i.e., $\tau = 0$ in eq 3. The calculated k_2^E value for **1e** falls on a single line with the experimental data for **1a–d** with excellent correlation. The Hammett ρ value is 1.8 ± 0.1 (Table 6).

For reactions of **1e** with $R_2NH/R_2NH_2{}^+$ buffer in 70 mol % MeCN(aq), the k_1 values increased but the k_{-1}/k_2 decreased as the basicity of the buffer increased. The plots of log k_1 and log k_{-1}/k_2 vs the pK_a values of the buffers were linear with excellent correlation (Figure S8). The slopes of the plots are 0.73 ± 0.04 and -0.19 ± 0.03, respectively.

To provide an additional evidence for the competing (E1cb)$_R$ mechanism, the H–D exchange experiment was carried out by mixing the reactants with i-Pr$_2$NH/i-Pr$_2$NH$_2{}^+$ buffer in 70 mol % MeCN–30% D$_2$O at -10 °C. The reactant was recovered immediately after mixing. The NMR spectrum of the recovered reactant indicated that approximately half of benzylic C–H bond was converted to the C–D bond.

Discussion

Reaction Mechanism and Transition State Structure for Eliminations from 1a–d and 2a–e Promoted by R_2NH in MeCN. Reactions of **1a–d** and **2a–e** with R_2NH in MeCN produced benzamides and aryloxide in nearly quantitative yields. The reactions proceed by the amine-promoted elimination to afford the ketenes followed by the addition of the R_2NH to the intermediate to afford the products. Addition–elimination mechanism ($B_{AC}2$) is ruled out by the negligible rates of aminolysis compared with the overall rates (Tables 1 and 2). A similar mechanism has been reported in closely related reactions.[17–21]

Under the reaction condition reported here, the ketene-forming eliminations from **1** and **2** must proceed either via a one-step concerted mechanism or via carbanion intermediates (free or ion-paired) in a stepwise mechanism as depicted in Scheme 1.[7]

The observed general base catalysis with the Brønsted β values ranging from 0.44 to 0.84 rule out the (E1cb)$_R$, (E1cb)$_{ip}$, and internal return mechanisms because these mechanisms would exhibit either a specific base catalysis or Brønsted β values near unity.[3,7] The possibility that the relatively large β values for eliminations from **1a–c** and **2b** are caused by the change to an E1cb mechanism is negated by the interaction coefficients, i.e., $p_{xy'} < 0$, $p_{xy} > 0$, and $p_{yy'} < 0$ (*vide infra*). In addition, the values of $|\beta_{lg}| = 0.41-0.50$ rule out a mechanism in which either k_1 [(E1cb)$_{irr}$] or k_d is rate limiting, for which a small or negligible leaving group effect is expected.[3,7] On the other hand, the results are consistent with an E2 mechanism in which there is partial cleavage of the C_β-H and C_α-OAr bonds in the transition state.

The structure of the transition states may be assessed by the Brønsted β, Hammett ρ, and β_{lg} values. The Brønsted β values indicate the extent of proton transfer in the transition state. For R_2NH-promoted eliminations from **1a–d** and **2a–e**, values of $\beta = 0.44-0.84$ were determined (Table 3). This indicates

(29) Coetzee, J. F. *Prog. Phys. Org. Chem.* **1965**, *4*, 45–92.

Reactions of Aryl Phenylacetates

J. Am. Chem. Soc., Vol. 119, No. 4, 1997 695

moderate to extensive cleavage of the C_β-H bonds in the transition states.

The extent of negative charge development in the transition state may be assessed with the Hammett ρ values. Surprisingly, however, the Hammett plots are curvilinear and show downward curvature (Figure 1). Causes for the curved Hammett plots have been attributed to (i) the change in mechanism, (ii) a single mechanism with a different extent of bond formation and cleavage in the transition state, and (iii) a different balance of polar and resonance effects by different substituents in the transition state.[30−32] Since the reactions of **1a−d** and **2a−e** with R_2NH in MeCN proceed by a common E2 mechanism (*vide supra*), possibility (i) can be ruled out. Possibility (iii) can also be negated because the resonance effect is already taken into account in the σ^- constants. In addition, the rate data showed excellent correlations with eq 3, i.e., $\rho = \rho_H + \tau\sigma^-$. Therefore, the observed ρ_H values of 3.5−2.0 for the ketene-forming eliminations can be interpreted with a significant negative charge development at the β-carbon in the transition states, which decreases gradually as the electron-withdrawing ability of the substituent increases (*vide infra*).

The β_{lg} values are usually taken as a qualitative measure of the extent of the leaving group cleavage. For Bz(i-Pr)NH-promoted eliminations from **1a−d**, the $|\beta_{lg}|$ values of 0.41−0.50 have been determined (Table 3). The results are consistent with limited extents of C_α-OAr bond cleavage in the transition states. Additional support for this conclusion is provided by the interaction coefficients, i.e., $p_{xy'} < 0$, $p_{xy} > 0$, and $p_{yy'} < 0$ (*vide infra*).

The combined results reveal that the ketene-forming eliminations from **1a−d** and **2a−e** proceed by the concerted E2 mechanism via an E1cb-like transition state with extensive C_β-H bond cleavage, significant negative charge development at the β-carbon, and limited C_α-OAr bond cleavage (*vide infra*). On the other hand, the reactions of aryl esters of phenylacetic acid with OH^- in 80% DMSO(aq) have been shown to proceed by the (E1cb)$_R$ or (E1cb)$_{ion-pair}$ mechanism.[18,20] The change in the elimination reaction mechanism for **1a** from (E1cb)$_R$ or (E1cb)$_{ion-pair}$ to E2 with the base−solvent system variation from OH^-−80% DMSO(aq) to R_2NH−MeCN can be attributed to a solvent effect. Since the negative charge that developed on the benzylic carbon in the E1cb intermediate cannot be stabilized by solvation in poorly anion-solvating MeCN, the activation energy for the E1cb mechanism should increase and the E2 mechanism may become the favored alternative.

Structure−Reactivity Coefficients. Changes in structure−reactivity parameters that reflect changes in the transition state structure can provide additional evidence for the mechanism of the elimination reactions.[7−11] These changes can usefully

(30) Young, P. R.; Jencks, W. P. *J. Am. Chem. Soc.* **1979**, *101*, 3288−3293.

(31) Drago, R. S.; Zoltewicz, J. A. *J. Org. Chem.* **1994**, *59*, 2824−2830 and references cited therein.

(32) (a) Yoshida, T.; Yano, Y.; Oae, S. *Terahedron* **1971**, *27*, 5343−5351. (b) Bunnett, J. F.; Sridharan, S.; Cavin, W. P. *J. Org. Chem.* **1979**, *44*, 1463−1471. (c) Hasan, T.; Sims, L. B.; Fry, A. *J. Am. Chem. Soc.* **1983**, *105*, 3967−3975.

(33) Cho, B. R.; Maing Yoon, C.-O.; Song, K. S. *Tetrahedron Lett.* **1995**, *36*, 3193−3196.

(34) A reviewer has made an interesting suggestion that the change of the solvent to more protic one would stabilize the upper left corner and the lower left products in Figure 3. This would produce perpendicular and parallel shifts whose resultant shows a marginal decrease in β and a decrease in $|\beta_{lg}|$ as is seen. However, we believe that the stabilization of the carbonyl oxygen atom by hydrogen bonding with $R_2NH_2^+$ in the buffer solution would have more profound influence on the transition state structure than can be described by the energy diagram.

(35) Cho, B. R.; Suh, Y. S.; Lee, S. J.; Cho, E. J. *J. Org. Chem.* **1994**, *59*, 3681−3682.
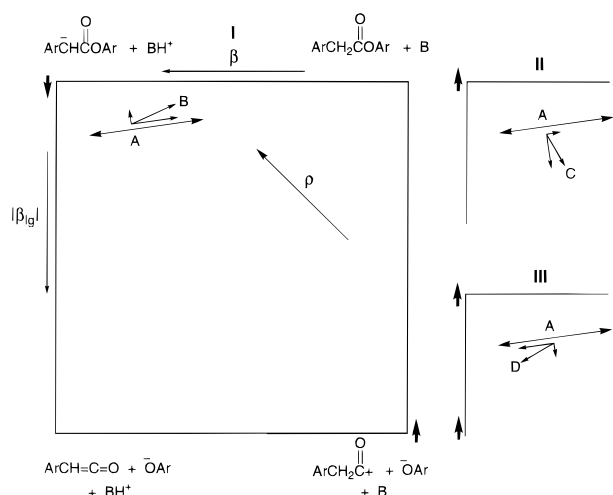

Figure 3. Reaction coordinate diagram for ketene-forming eliminations. The effects of the change to a stronger electron-withdrawing substituent, a better leaving group, and a weaker base are shown by the shift of the transition state from A to B, A to C, and A to D in I, II, and III, respectively.

be described on energy surface of More-O'Ferall−Jencks diagram.[7,8] An energy surface for the elimination reactions of R_2NH-promoted eliminations from **1a−d** and **2a−e** in MeCN is shown in Figure 3.

Table 3 shows that the Brønsted β values for R_2NH-promoted eliminations from **1a−d** and **2a−e** decrease as the electron-withdrawing ability of the β-phenyl substituent is increased. The results can be described by a negative $p_{xy'}$ interaction coefficient, $p_{xy'} = \partial\beta/\partial\sigma = \partial\rho/\partial pK_{BH}$, that describes the interaction between the base catalyst and the β-aryl substituent.[7,8] Negative $p_{xy'}$ coefficients are consistent with an (E1cb)$_{irr}$ mechanism, which has been ruled out by the substantial values of the $|\beta_{lg}|$ (*vide supra*) and an E2 mechanism and a reaction coordinate with a large horizontal component corresponding to proton transfer.[7−11] These changes in the β values can be described on More-O'Ferrall−Jencks energy diagram (Figure 3). An electron-withdrawing β-aryl substituent will lower the energy of the carbanion intermediate in the upper left corner of the energy diagram. The transition state on the horizontal reaction coordinate will then move toward the right, with less proton transfer and a smaller β, as depicted by a shift from A to B in Figure 3I.[8]

For all β-aryl substituents the Brønsted β values decrease as the leaving group is changed from 4-nitrophenoxide to 2,4-dinitrophenoxide (Table 3). This effect corresponds to a positive p_{xy} interaction coefficient, $p_{xy} = \partial\beta/\partial pK_{lg} = \partial\beta_{lg}/\partial pK_{BH}$, that describes the interaction between the base catalyst and the leaving group.[7,8] The observed increase in the $|\beta_{lg}|$ values as the catalyst is made less basic (Table 4) is another manifestation of this effect, i.e., $p_{xy} = \partial\beta_{lg}/\partial pK_{BH} > 0$.[7,8] On the More-O'Ferrall−Jencks reaction coordinate diagram in Figure 3, a change to a better leaving group will raise the energy of the top edge of diagram. The transition state on the horizontal reaction coordinate would then move slightly toward the right as depicted by a shift from A to C on the energy diagram, resulting in a small decrease in β (Figure 3II).[8] Similarly, a weaker base will raise the energy of the left side of the diagram and shift the transition state from A to D to increase in the extent of C_α-OAr bond cleavage (Figure 3III).[8] The positive p_{xy} coefficients are not consistent with an E1cb mechanism for which $p_{xy} = 0$ is expected, but provide additional support for the concerted E2 mechanism.[7−11]

As shown in Table 3, there is a progressive decrease in the $|\beta_{lg}|$ values as the β-aryl substituent is changed from *p*-MeO to

H to *m*-Cl to *m*-NO$_2$. This result can be described by a negative $p_{yy'}$ interaction coefficient, $p_{yy'} = -\partial\beta_{lg}/\partial\sigma^- = -\partial\rho/\partial pK_{lg}$, that describes the interaction between the leaving group and the β-aryl substituent.[7,8] The decrease in the ρ_H values with a better leaving group (Table 4) provides additional evidence for this effect, i.e., $p_{yy} = -\partial\rho_H/\partial pK_{lg} < 0$.[7,8] The negative $p_{yy'}$ coefficients observed in these reactions are consistent an E2 mechanism and a reaction coordinate that has a large component of proton transfer so that stabilization of the carbanion intermediate result in a net shift from A to B in Figure 3I, in the direction of decreased C$_\alpha$-OAr bond cleavage and smaller $|\beta_{lg}|$ values.[7–11] Moreover, a better leaving group would shift the transition state from A to C in Figure 3II to decrease the extent of negative charge development and the ρ_H values.[8]

Solvent Effect. The observed second-order kinetics with the Brønsted $\beta = 0.77$ and $\beta_{lg} = -0.26$ for the amine-promoted eliminations from **1a** in 70 mol % MeCN(aq) (Table 6) reveal that the reactions also proceed by the concerted E2 mechanism. Moreover, the decrease in the β values with a stronger electron-withdrawing β-aryl substituent (Table 3), i.e., $p_{xy'} < 0$, is consistent with an E2 mechanism and a reaction coordinate with a large component of proton transfer (*vide supra*).

For eliminations from **1** promoted by *i*-Pr$_2$NH, the rate decreases only slightly as the base−solvent system is changed from *i*-Pr$_2$NH−MeCN to *i*-Pr$_2$NH/*i*-Pr$_2$NH$_2$$^+$−70 mol % MeCN−30% H$_2$O, apparently because of the decreased basicity of the promoting base in more protic solvent.[25,31] On the other hand, the extent of C$_\beta$-H bond cleavage decreases slightly and the degrees of negative charge development at the β-carbon and the C$_\alpha$-OAr bond cleavage decrease considerably as revealed by the small to significant decrease in the Brønsted β, ρ, and $|\beta_{lg}|$ values in R$_2$NH/R$_2$NH$_2$$^+$−70 mol % MeCN(aq) as the base−solvent system (Table 6). The changes in the transition state structures with the base−solvent system variation may be attributed to a solvent effect. Due to the electronegativity difference, the negative charge developed at the β-carbon in the ketene-forming transition state may be delocalized more on the carbonyl oxygen than on the β-carbon. Moreover, this effect would be amplified in the buffer solution because the former can be better stabilized by forming a stronger hydrogen bond with R$_2$NH$_2$$^+$. This would predict that less negative charge would remain at the β-carbon to decrease both ρ_H and $|\beta_{lg}|$ values, as observed.[36]

Appearance of Concurrent E2 and E1cb Mechanisms. Figure 2 shows a plot of k_{obs} vs free buffer concentration for eliminations from **1e** promoted by *i*-Pr$_2$NH/*i*-Pr$_2$NH$_2$$^+$ buffer in 70 mol % MeCN(aq). The plots are curvilinear at low buffer concentration but become straight lines at [buffer] > 0.01 M for all buffer systems employed (Figure S4−S6). This result cannot be explained with the change in the rate-limiting step because the rate should have reached a plateau at a higher buffer concentration in such a case. On the other hand, the rate data can readily be analyzed with a nonlinear regression analysis by assuming that the reactions proceed by concurrent E2 and E1cb mechanisms (eq 4). The excellent correlations of the experimental data with the computer-fitted curves demonstrate the reliability of the kinetic analysis. In addition, the shapes of the dissected lines are typical for the E2 and E1cb reactions, respectively (Figure 2).

Figure S7 shows that the calculated k_2^E value for eliminations from **1e** falls on a single line with the experimental data for **1a−d** in the Hammett plot. This result provides a strong support that the k_2^E pathway for **1e** and elimination reactions of **1a−d**

(36) Cho, B. R.; Lee, S. J.; Kim, Y. K. *J. Org. Chem.* **1995**, *60*, 2072−2076.

proceed by the common E2 mechanism. In addition, the Brønsted β value determined with the calculated k_2^E value for **1e** is 0.66, which is smaller than that of 0.77 for **1a** (Table 3). This corresponds to a negative $p_{xy'}$ interaction coefficient and provides additional support for the operation of the E2 mechanism in the k_2^E process for **1e** and a reaction coordinate that has a large component of proton transfer (*vide supra*).[7–11]

The calculated k_1 and k_{-1}/k_2 values provide strong evidence for the existence of the stepwise E1cb mechanism. The k_1 value increases with a stronger base apparently because it involves the cleavage of the C$_\beta$-H bond leading to the carbanion intermediate. The large β value of 0.73 for the k_1 step is also reasonable because the C$_\beta$-H bond should be extensively broken in the transition state. Moreover, the slope of the plot of log k_{-1}/k_2 vs pK_a values of the buffer is −0.19 (Figure S8). Although the k_2 value should be independent of the basicity because it is an intramolecular process, the k_{-1} should decrease as the R$_2$NH$_2$$^+$ becomes a weaker acid. Hence the slope of this plot could be taken as a measure of the extent of proton transfer from the R$_2$NH$_2$$^+$ to the carbanion in the k_{-1} step. The small negative slope is consistent with a reactant-like transition state for the k_{-1} step and provides additional support for the stepwise E1cb mechanism. Finally, the H−D exchange experiment reveals that approximately half of the benzylic C−H bond in the recovered starting material has been converted to the C−D bond in 70 mol % MeCN−30% D$_2$O. All of these results are in excellent agreement with concurrent E2 and E1cb mechanisms for the reaction of **1e** with R$_2$NH/R$_2$NH$_2$$^+$ buffers in 70 mol % MeCN(aq).

It has been argued that the change in mechanism from E2 to E1cb for eliminations from (2-arylethyl)ammonium ions and 9-(2-X-2-propyl)fluorenes occurs by the merging of the transition states because it is difficult for the energy maximum for the transition state of the E2 reaction and an energy well for the E1cb reaction to coexist for a single compound at almost the same position on the energy diagram.[9,12] However, if the energies of the transition states for the competing reactions are similar and if the positions of transition states on the energy diagram are significantly different and/or if there is sufficient energy barrier between them, they should be able to coexist. For example, clear evidences for the concurrent E2 and E1 mechanisms have been reported for the methoxide-promoted eliminations from 2-chloro-2-methyl-1-phenylpropanes and *N*-(arylsufonoxy)-*N*-alkylbenzylamines as well as for the solvolytic eliminations of 9-(1-X-ethyl)fluorenes.[13–15] The mechanistic borderline observed in the ketene-forming elimination from **1e** is concluded to be of the second type. Thus the elimination reactions of **1a−d** with R$_2$NH in MeCN proceed by an E2 mechanism (*vide supra*). The mechanism changes from E2 to the parallel E2 and E1cb mechanisms by the introduction of the *p*-NO$_2$ group at the β-aryl ring and the R$_2$NH/R$_2$NH$_2$$^+$ buffer in 70 mol % MeCN(aq) as the base−solvent system, probably because the E1cb intermediate is stabilized by such changes so that the two mechanisms can coexist. The transition states for the two reactions appear to be appreciably separated on the energy surface as indicated by the significant increase in the β value from 0.66 for the E2 to 0.73 for the k_1 step of the E1cb mechanism, respectively (Table 3). A further stabilization of the carbanion intermediate by utilizing OH$^-$−80% DMSO(aq) as the base−solvent system induces a change in the reaction mechanism to an E1cb (Table 7). To our knowledge, this is the first example that clearly demonstrates that the E2 mechanism changes to an E1cb via concurrent E2 and E1cb mechanisms.

Table 7. Kinetic Parameters for Various Elimination Reactions

reaction	kinetic order	β	$|\beta_{lg}|$	mechanism	ref
$C_6H_5CH_2CO_2C_6H_4$-p-NO_2 + R_2NH in MeCN	2	0.82	0.4−0.5	E2	this work
p-$O_2NC_6H_5CH_2CO_2C_6H_4$-p-NO_2 + $R_2NH/R_2NH_2^+$ in 70 mol % MeCN(aq)	1−2	0.66−0.77	0.26	E2 and E1cb	this work
$C_6H_5CH_2CO_2C_6H_4X$ + OH^- in 80% DMSO(aq)	1−2		0.65	$(E1cb)_R$ or $(E1cb)_{ion\ pair}$	18
p-$O_2NC_6H_5CH_2CO_2C_6H_4X$ + OH^- in 80% DMSO(aq)	1		1.25, 1.34[a]	$(E1cb)_{anion}$	18, 20
$C_6H_5NHCO_2C_6H_4X$ + OH^- in H_2O	1		1.34	$(E1cb)_{anion}$	22g

[a] Calculated with the rate data in ref 20 and the estimated pK_{lg} values in ref 18.

Experimental Section

Materials. Aryl esters of arylacetic acids **1** and **2** and of alkanoic acids **3** and **4** were prepared by reactions of appropriately substituted arylacetic acids and alkanoic acids with phenols in toluene or CH_2Cl_2 in the presence of 2-chloro-1-methylpyridinium iodide.[23] The physical, spectral, and analytical data for these compounds were consistent with the proposed structures. The melting point (°C), NMR (ppm), IR (cm^{-1}), and combustion analysis data of the new compounds are listed in the Supporting Information.

Acetonitrile was purified, and solutions of R_2NH in MeCN were prepared as described before.[5] The buffer solutions of $R_2NH_2^+/R_2NH$ in 70 mol % MeCN(aq) were prepared by adding equivalent amounts of $R_2NH_2^+$ and R_2NH to 70 mol % MeCN(aq). In all cases, the buffer ratio was maintained to be 1.0.

Kinetic Studies. Reactions of **1−4** with R_2NH in MeCN or $R_2NH/R_2NH_2^+$ buffer in 70 mol % MeCN(aq) were followed by monitoring the increase in the absorption of the aryl oxides at 400 and 426 nm with a UV−vis spectrophotometer as described before.[5,6,35] Reactions of **2e** with R_2NH in MeCN and of **1e** with $R_2NH_2^+/R_2NH$ buffer in 70 mol % MeCN(aq) were too fast to be measured by this method, so the rate studies utilized a stopped-flow spectrophotometer.

Buffer Association. For reactions of **1e** with $R_2NH/R_2NH_2^+$ buffer in 70 mol % MeCN(aq), the plots of k_{obs} vs buffer concentration showed downward curvature. The negative deviation may be accounted for by buffer association forming kinetically inactive hydrogen-bonded complexes, $R_2NH_2^+\cdots NHR_2$. The buffer association constants K_{assoc} were determined as described in the literature[26] by using eq 5, where $[B^-]_{ST}$ and $[BH]_{ST}$ are the stoichiometric concentrations of the buffer components and $[B^-]$ represents the concentration of the free amine base. The K_{assoc} values are 6.5, 6.0, 7.3, and 20 for Bz(i-Pr)NH, (i-

$$K_{assoc} = [B^-\cdots BH]/[B^-][BH] = ([B^-]_{ST} - [B^-])/([BH]_{ST} -$$
$$[B^-\cdots BH])([B^-]_{ST} - [B^-\cdots BH]) \quad (5)$$

Bu)$_2$NH, i-Pr$_2$NH, and 2,6-dimethylpiperidine buffers, respectively. Utilizing these values, $[B^-]_{ST}$, and $[BH]_{ST}$ the free buffer concentration was calculated for all buffers prior to analysis of the kinetic data.

Calculation of the k_2^E, k_1, and k_{-1}/k_2 Values. Utilizing the k_{obs} values and the free buffer concentration, the k_2^E, k_1, and k_{-1}/k_2 values that best fit with eq 4 have been calculated with the NLSFIT function in the GENPLOT program, which is a nonlinear square fitting routine based on the gradient search and function linearization method.[27]

Product Studies. The yields of the aryloxides determined by comparing the absorbance of the infinity samples from the kinetic reactions with those of authentic aryloxides were in the range 92−

98%. To determine the yields of *N,N*-diisopropylbenzamide by GC, **1a** and **2a** (0.08 mmol) were reacted with 10 equiv of i-Pr$_2$NH in 5 mL of MeCN for 2 h. After evaporation of the solvent, the product was taken up in CH_2Cl_2 and washed thoroughly with water until all of the amine, ammonium salt, and the aryloxides were completely removed. The products were analyzed by GC as described before.[35] The yields of *N,N*-diisopropylbenzamide from the reactions of **1a** and **2a** were 88 and 92%, respectively. The reaction of **1a** and **2a** with i-Pr$_2$NH/i-Pr$_2$NH$_2^+$ in 70 mol % MeCN(aq) were conducted by the same procedure except that smaller amount of the reactants (ca. 0.01 mmol) were used. The products were identified by TLC and NMR. The products were *N,N*-diisopropylbenzamide and phenylacetic acid.

H−D Exchange Experiment. To determine whether **1e** may undergo H−D exchange reaction, **1e** (0.059 g, 0.19 mmol) was added to 3.4 mL of i-Pr$_2$NH/i-Pr$_2$NH$_2^+$ buffer in 70 mol % MeCN−30% D_2O at −10 °C. The reaction was quenched by adding dilute D_2SO_4 in D_2O immediately after mixing. The recovered reactant was isolated by extracting the products with ethyl acetate followed by the silca gel column chromatography using ethyl acetate/hexane = 1/4 as eluent. The proton NMR spectrum of the recovered reactant was identical to that of **1e** except that the integration at δ 4.08 was decreased by approximately 50%.

Control Experiments. The stability of **1−2** were determined as reported earlier.[5,6] They were stable for at least 3 weeks in MeCN solution at room temperature.

Supporting Information Available: List of melting point (°C), NMR (ppm), IR (cm^{-1}), and combustion analysis data of the new compounds, Charton plot for aminolysis of **4a−d** with i-Pr$_2$NH in MeCN, plot of k_{obs} vs [buffer] for eliminations from **1a** promoted by i-Pr$_2$NH/i-Pr$_2$NH$_2^+$ in 70 mol % MeCN(aq) at 25.0 °C, plots of k_{obs} vs [buffer] for ketene-forming eliminations from **1e** promoted by R_2NH in MeCN and $R_2NH/R_2NH_2^+$ in 70 mol % MeCN(aq) at 25.0 °C, Hammett plot for eliminations from **1a−e** promoted by i-Pr$_2$NH/i-Pr$_2$NH$_2^+$ buffer in 70 mol % MeCN(aq) at 25.0 °C, plot of log k_1 and log k_{-1}/k_2 vs pK_a of the buffers for eliminations from **1e** promoted by $R_2NH/R_2NH_2^+$ in 70 mol % MeCN(aq) at 25.0 °C (10 pages). See any current masthead page for ordering and Internet access instructions.

JA961294K